

One-dimensional consolidation under haversine repeated loading with rest period

Sabah S. Razouki · Tom Schanz

Received: 29 September 2009 / Accepted: 13 December 2010 / Published online: 3 February 2011
© Springer-Verlag 2011

Abstract Presented in this paper is a study of the one-dimensional consolidation process under haversine repeated loading with and without rest period. The analysis was carried out using a hybrid coupled, analytical and numerical implicit finite difference technique. The rate of imposition of excess pore-water pressure was determined analytically, and the remaining part of the governing differential equation was solved numerically. The clay deposit considered was a homogeneous clay layer with permeable top and/or impermeable bottom hydraulic boundary conditions with constant coefficients of permeability and of consolidation. The study reveals that although the loading function is positive for all times, the excess pore-water pressure at the base of the clay deposit with permeable top and impermeable bottom oscillates with time reaching a ‘steady state’ after few cycles of loading depending on whether there is a rest period or not. An increase in the rest period causes a decrease in the number of cycles required to achieve the steady state. The paper shows also that the rest period in the haversine repeated loading decelerates the consolidation process. Similarly, the paper reveals that the effective stress at the bottom of the clay layer with permeable top and impermeable bottom increases with time but showing mild fluctuations that do not change the sign. The maximum positive effective stress achieved depends on the rest period of the haversine repeated loading. A haversine

repeated loading without a rest period gives the highest value for the positive effective stress.

Keywords Consolidation · Haversine repeated loading · Hybrid analytical and numerical solution

Notation

A	Coefficient matrix
a	Radius of circular tire-pavement contact area; constant quantity
B	Column vector of unknown quantities
C	Column vector of known quantities
C_z	Coefficient of consolidation in vertical direction
d	Period of haversine repeated loading without rest period or the duration of loading/unloading phase of the haversine repeated loading with rest period
H	Thickness of clay layer with permeable top and impermeable bottom or half the thickness of a clay layer with permeable top and bottom
k	Number of uniform intervals Δz in H
L	Loading function (haversine repeated loading with or without rest period)
m	Integer
n^*	Number of uniform intervals Δt within (d)
PTIB	Clay layer with permeable top and impermeable bottom
PTPB	Clay layer with permeable top and bottom
q	Amplitude of haversine repeated loading
R	Rest period
S	Function of time
s	Speed of vehicle for highways or airports
T_v	Dimensionless time factor
t	Actual time
u	Excess pore-water pressure
u_e	Imposed excess pore-water pressure

S. S. Razouki · T. Schanz (✉)

Faculty of Civil and Environmental Engineering Chair for Foundation Engineering, Soil & Rock Mechanics, Ruhr-Universität, Bochum, Germany
e-mail: tom.schanz@rub.de

z	Vertical coordinate measured from top surface of the clay layer downward positive
β	Dimensionless coefficient in implicit finite difference equation
σ'	Effective stress

1 Introduction

Some of the most important applications of repeated loading take place in highway, airport, and railway engineering. In such types of geotechnical structures, the roadbed soil (subgrade soil) behavior depends upon the time-dependent behavior of the repeated loading.

Mitchell [12] pointed out that repeated or cyclic loading of soils may result from a number of natural phenomena or human activities such as vehicular traffic, wind waves, reciprocating machinery, and others.

Conte and Troncone [3] reported that special structures such as silos or fluid tanks subject the soils to loading and unloading stages that repeat themselves more or less periodically over time.

Many forms of time-dependent behavior of repeated loading were suggested by various authors [2, 9, 11].

Barksdale [2] pointed out that the stress pulse can be approximated by a haversine or a triangular function. However, McLean [11] determined the loading time for an equivalent square wave vertical pulse. Huang [9] pointed out that the type and duration of loading used in the repeated load test should simulate that actually occurring in the field, and he recommended the use of a stress pulse in the form of a haversine or triangular loading.

2 Characteristics of loading waveform

For highways and airports, Huang [9] reported that when a wheel load is at a considerable distance from a given point

in the pavement, the stress at that point is zero and when the load becomes directly above the point considered, the stress at that point is maximum. Therefore, it is reasonable to assume the stress pulse to be a haversine or triangular loading, the duration of which depends on the vehicle speed tire contact radius as well as the depth of the point below the surface of the flexible or rigid pavement.

Huang [9] reported that a reasonable assumption is that the load has practically no effect when it is at a distance of six times the radius of the circular tire-pavement contact area from the point considered. This means that

$$d = 12 \frac{a}{s} \quad (1)$$

where d = duration of the load, a = radius of circular tire-pavement contact area, s = vehicle speed.

Huang [9] recommended the use of the following haversine loading given by

$$L(t^*) = q \sin^2 \left(\frac{\pi}{2} + \frac{\pi t^*}{d} \right) \quad (2)$$

where $L(t^*)$ = loading as a function of time, q = load amplitude, t^* = time, d = period of repeated load.

For $t = t^* + d/2$, it can be shown easily that (see Fig. 1):

$$L(t) = q \sin^2 \frac{\pi t}{d} \quad (3)$$

and

$$\frac{dL(t)}{dt} = \frac{q\pi}{d} \sin \frac{2\pi t}{d}. \quad (4)$$

3 Duration of loading and rest period

It is well known that the vehicle speed varies a great deal, and the depth of the material may not be known during the design stage. For these reasons, Huang [9] recommended the use of duration of 0.1 s and a rest period of 0.9 s.

It is worth mentioning that the load duration has very little effect on the resilient modulus of granular soils, but it

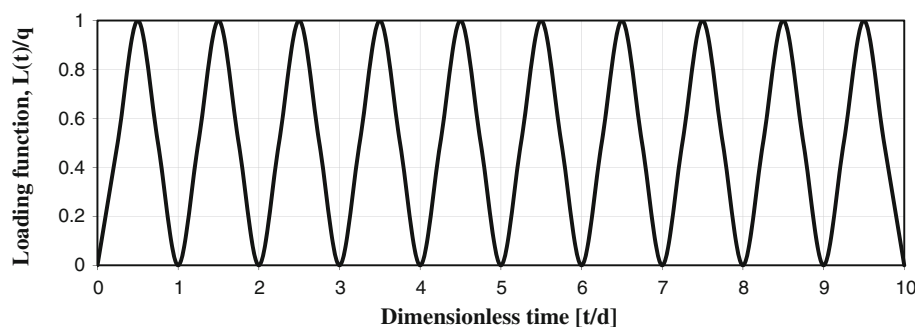


Fig. 1 Haversine loading function

has some effect on fine-grained soils depending on moisture content. Huang [9] stated that the effect of rest period is not known, and it is probably insignificant. However, the effect of rest period of repeated loading on the consolidation process is one of the main objects of this paper, and it will be discussed thoroughly under Sect. 8.

4 Governing differential equation for 1-D consolidation

It is well known that the Terzaghi one-dimensional theory of consolidation under instantaneous loading was borne in 1923 and published in his books in 1925 and 1943 [16, 17]. Terzaghi and Fröhlich [15] extended the Terzaghi theory to various cases of time-dependent loading following a single ramp loading. Olson [13] presented charts for one-dimensional consolidation for the case of simple ramp loading assuming constant coefficient of consolidation. Hsu and Lu [8] extended Olson's solution of one-dimensional consolidation to those with varying loading-dependent coefficients of consolidation. Conte and Troncone [3] presented analytical solution for the analysis of one-dimensional consolidation of saturated soil layers subjected to general time-dependent loading including the cases of cyclic square wave and trapezoidal loadings. Their solution was in agreement with Baligh and Levadaux [1] for 1-D consolidation for the case of repeated rectangular loading. However, Favaretti and Soranzo [5], Guan et al. [7] and Geng et al. [6] derived some solutions for different types of cyclic loadings. For example, Geng et al. [6] developed a simple semi-analytical method to solve the one-dimensional non-linear consolidation problems with variable compressibility and permeability under cyclic loadings. They presented the Laplace Transform for suddenly imposed constant loading, rectangular pulse cyclic loading,

sinusoidal cyclic loading, triangular cyclic loading, and trapezoidal cyclic loading. However, no experimental results were presented for any case of cyclic loadings.

Zimmerer [19] treated also the problem of 1-D consolidation under sinusoidal loading only using finite difference technique. He extended his study to nonlinear 1-D consolidation taking into account nonlinear variation in permeability and density, and allowance was made for geometrical non-linearity.

Razouki and Al-Zayadi [14] extended the consolidation study to time-dependent embankment loading and presented various charts for quick use in practice taking into account anisotropic permeability, various shapes of the embankment loading, various clay layer thicknesses relative to the base width of the embankment and various construction periods.

The governing differential equation adopted in this work is that of Terzaghi and Fröhlich for time-dependent loading as follows (see Fig. 2):

$$\frac{\partial u}{\partial t} = C_z \frac{\partial^2 u}{\partial z^2} + \frac{\partial u_e}{\partial t} \quad (5)$$

where $u(z, t)$ = excess pore-water pressure at the position z and time t , C_z = coefficient of consolidation in vertical z -direction, $u_e(t)$ = imposed excess pore-water pressure at time t .

For the case of a haversine wave, as given by Eq. 3 and noting that $u_e = L(t)$ and that $\partial u_e / \partial t = dL/dt$, the governing differential equation becomes:

$$\frac{\partial u}{\partial t} = C_z \frac{\partial^2 u}{\partial z^2} + \frac{q\pi}{d} \sin \frac{2\pi t}{d}. \quad (6)$$

It should be noted at this stage that the coefficient of swelling is assumed to be equal to that of consolidation for the purpose of this work. This is quite justified for over

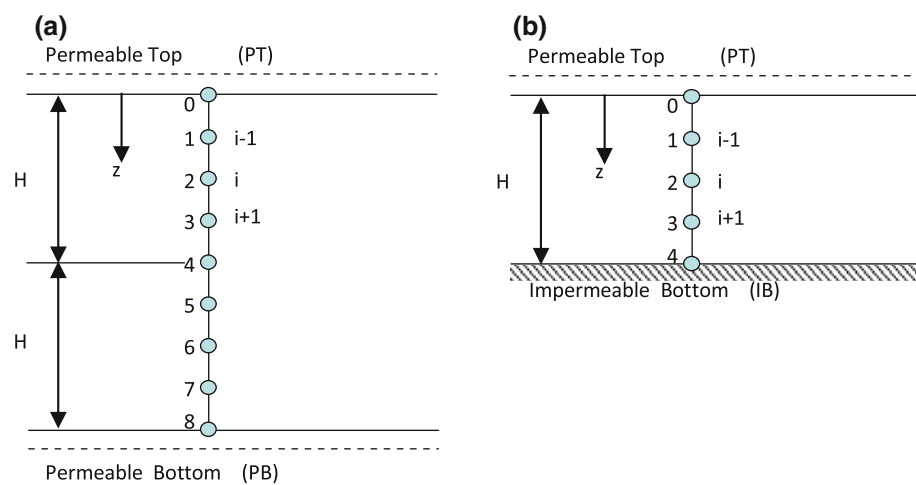


Fig. 2 Clay layer **a** with permeable top and bottom **b** with permeable top and impermeable bottom

consolidated clays as well as for loading/unloading cycles of normally consolidated clays.

5 Analytical solution of governing differential equation

The governing differential Eq. 6 is a non-homogeneous partial differential equation. The solution of this differential equation consists of two parts. The first part of this solution represents the solution of the homogeneous differential equation, while the second part represents the particular integral of the non-homogeneous equation. It is worth mentioning that such an exact analytical solution could not be found in common references on advanced engineering mathematics [4, 10, 18]. However, such a solution is possible to obtain in terms of infinite series of eigenfunctions, but it is somewhat cumbersome to achieve at this stage and it will be devoted to another paper on this subject.

Therefore, it was decided at this stage to develop a numerical finite difference solution for this work to arrive at the behavior of the consolidation process under haversine loading.

6 Numerical solution of governing differential equation

To solve the governing differential equation, the implicit finite difference technique is to be used. For this purpose, the case of a clay layer with permeable top and permeable bottom (PTPB case), having a total thickness of $2H$ or a clay layer with permeable top and an impermeable bottom (PTIB case) having a thickness of H as shown in Fig. 2, is considered.

Four uniform intervals Δz are to be used together with a uniform time step Δt . Thus, the implicit finite difference approximation for the governing partial differential Eq. 6 becomes:

$$\frac{u_{i,n+1} - u_{i,n}}{\Delta t} = C_z \frac{u_{i-1,n+1} - 2u_{i,n+1} + u_{i+1,n+1}}{(\Delta z)^2} + \frac{q\pi}{d} \sin \frac{2\pi t}{d} \quad (7)$$

where $u_{i,n}$ = excess pore-water pressure at node (i) and time level (n), $u_{i,n+1}$ = excess pore-water pressure at node (i) and time level ($n+1$), $u_{i-1,n+1}$ = excess pore-water pressure at node ($i-1$) and time level ($n+1$), $u_{i+1,n+1}$ = excess pore-water pressure at node ($i+1$) and time level ($n+1$).

It can be shown easily that the above equation can be simplified to the following form:

$$-\beta u_{i-1,n+1} + (1 + 2\beta)u_{i,n+1} - \beta u_{i+1,n+1} = u_{i,n} + \frac{q\pi}{n^*} \sin \frac{\pi(2m-1)}{n^*} \quad (8)$$

where

$$\beta = \frac{C_z \Delta t}{(\Delta z)^2} = k^2 \Delta T_v \quad (9)$$

k = number of uniform intervals Δz in H , T_v = dimensionless time factor $= c_z t / H^2$, n^* = number of uniform time intervals (Δt) within one cycle (d), t = actual time $= m \Delta t$, $m = 1, 2, 3, \dots$

Note that the imposed time-dependent loading was taken at the middle of the time step.

For the case of four uniform intervals Δz within H (i.e. $k = 4$), the governing matrix equation becomes for $q = \text{unity}$:

$$\begin{bmatrix} 1 + 2\beta & -\beta & 0 & 0 \\ -\beta & 1 + 2\beta & -\beta & 0 \\ 0 & -\beta & 1 + 2\beta & -\beta \\ 0 & 0 & -2\beta & 1 + 2\beta \end{bmatrix} \begin{bmatrix} u_{1,n+1} \\ u_{2,n+1} \\ u_{3,n+1} \\ u_{4,n+1} \end{bmatrix} = \begin{bmatrix} u_{1,n} + a \sin[a(2m-1)] \\ u_{2,n} + a \sin[a(2m-1)] \\ u_{3,n} + a \sin[a(2m-1)] \\ u_{4,n} + a \sin[a(2m-1)] \end{bmatrix}$$

$$\text{or } A B = C, B = A^{-1} C \quad (10)$$

where $a = \pi/n^*$.

A = coefficient matrix =

$$\begin{bmatrix} 1 + 2\beta & -\beta & 0 & 0 \\ -\beta & 1 + 2\beta & -\beta & 0 \\ 0 & -\beta & 1 + 2\beta & -\beta \\ 0 & 0 & -2\beta & 1 + 2\beta \end{bmatrix}.$$

B = vector of unknown quantities $= [u_{1,n+1} \ u_{2,n+1} \ u_{3,n+1} \ u_{4,n+1}]^T$.

C = vector of known quantities $= [u_{1,n} + S \ u_{2,n} + S \ u_{3,n} + S \ u_{4,n} + S]^T$

$$S = a \sin[a(2m-1)]. \quad (10a)$$

A^{-1} = inverse of the coefficient matrix.

7 Application

For the clay deposit shown in Fig. 2, the choice of a dimensionless time interval ΔT_v of 0.025, together with $k = 4$, yields according to Eq. 9 a β -value of 0.4. For $\beta = 0.4$, $k = 4$ and $n^* = 6$ (i.e. the period d is divided into six uniform time intervals), it can be shown easily that

$$A = \begin{bmatrix} 1.8 & -0.4 & 0 & 0 \\ -0.4 & 1.8 & -0.4 & 0 \\ 0 & -0.4 & 1.8 & -0.4 \\ 0 & 0 & -0.8 & 1.8 \end{bmatrix},$$

$$A^{-1} = \begin{bmatrix} 0.5852 & 0.1378 & 0.3398 & 0.0076 \\ 0.1378 & 0.6202 & 0.1529 & 0.0340 \\ 0.0340 & 0.1529 & 0.6541 & 0.1454 \\ 0.0151 & 0.6800 & 0.2907 & 0.6202 \end{bmatrix}.$$

Thus, the solution at any time t can be obtained easily using the inverse matrix given above.

Figure 3 shows the time variation of ‘excess’ pore-water pressure at the bottom of the clay deposit with permeable top and impermeable bottom given in Fig. 2.

It is quite obvious that the ‘excess’ pore-water pressure builds up during the loading phase and changes to negative pore-water pressure during the unloading phase. This oscillation continues with some damping until a ‘steady’ state is achieved after about eight cycles. This can be supported by the fact that the ratio of positive amplitude of the first cycle of the excess pore-water pressure at the bottom of the PTIB case to that for the second cycle is about 1.136, while this ratio becomes, for example, about 1.048 for the ratio corresponding to the sixth’s and seventh’s cycle. Similarly, Fig. 4 shows the ‘excess’ pore-water pressure isochrones for the PTIB case considered for different values of the dimensionless time factor T_v during the loading and unloading phases of the first cycle of the haversine loading. It is quite obvious that during loading, the excess pore-water pressure isochrones are positive changing gradually to negative isochrones during the unloading phase of the haversine loading. Note that the ‘excess’ pore-water pressure isochrones can be partially negative and partially positive. Figure 5 shows the time variation of the effective stress during the cycles studied. It is quite obvious from this figure that the effective stress increases, in general, with time but showing some light fluctuation (without changing sign) due to the loading–unloading phases of the cyclic loading. This means that the bearing capacity of the soil increases, in general, gradually with increasing number of cycles of the repeated loading. The rate of increase in effective stress is pronounced

initially and dies out thereafter, and a steady state may be achieved after about 8 cycles.

8 Effect of rest period

To study the effect of rest period on the one-dimensional consolidation process under repeated loading, the haversine loading wave shown in Fig. 6 is considered. It is obvious from this figure that the duration of the haversine loading–unloading phase is given by (d) , while the rest period is given by (R) . Thus, this repeated loading is a periodic function given in the fundamental period as follows:

$$L(t) = \begin{cases} 0 & \text{for } 0 \leq t \leq R/2 \\ q \sin^2 \pi/d(t - R/2) & \text{for } R/2 \leq t \leq d + R/2 \\ 0 & \text{for } d + R/2 \leq t \leq d + R \end{cases}. \quad (11)$$

The first time derivative of this loading function representing the rate of imposition of excess pore-water pressure can be written as follows:

$$\frac{dL}{dt} = \begin{cases} 0 & \text{for } 0 \leq t \leq R/2 \\ q\pi/d \sin 2\pi/d(t - R/2) & \text{for } R/2 \leq t \leq d + R/2 \\ 0 & \text{for } d + R/2 \leq t \leq d + R \end{cases}. \quad (12)$$

Thus, the analysis of the one-dimensional consolidation process can proceed as before.

The same case treated earlier (see Fig. 2) was analyzed again but using the haversine loading wave given by Eq. 11 and shown in Fig. 6 assuming $R/d = 1$ to reveal the effect of rest period on the one-dimensional consolidation process.

Figure 7 shows the time variation of ‘excess’ pore-water pressure at the impermeable base of the clay layer for the

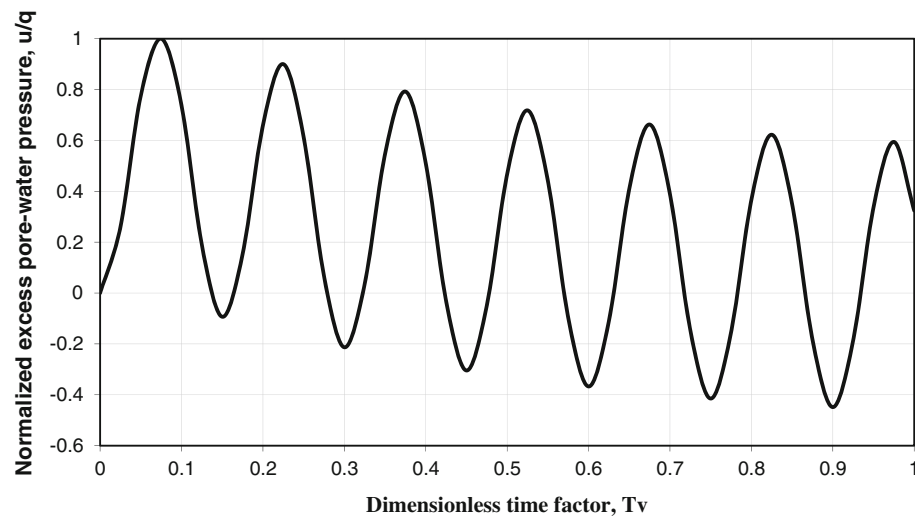


Fig. 3 Time variation of “excess” pore-water pressure at the bottom of a clay layer with permeable top and impermeable bottom

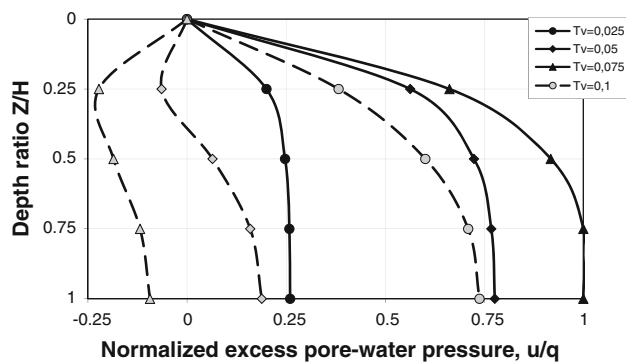


Fig. 4 “Excess” pore-water pressure isochrones for the PTIB case during the first haversine loading cycle

case of a haversine loading with a rest period $R = d$. Included also in this figure are the corresponding data for the cases $R/d = 0$ and $R/d = 2$. Note that for the case of zero rest period, the loading/unloading time covers the whole cycle length, while for the case of a rest period $R = d$ or $R = 2d$, the duration of loading/unloading becomes relatively short relative to the cycle length. Thus, the existence of an ‘effective’ gradient for longer time in the case of zero rest period when compared with that for non-zero rest period might explain why the positive excess pore-water pressure peaks in Fig. 7 increase with increasing R/d ratio. Thus, the increase in the rest period decelerates the consolidation process. It is also worth noting that

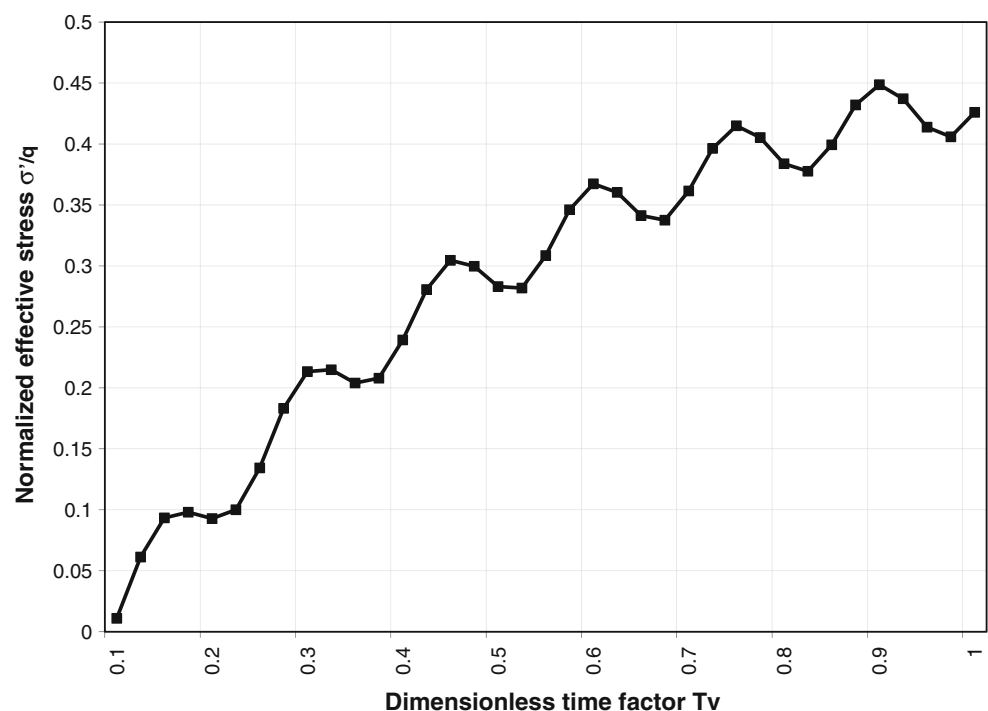


Fig. 5 Time variation of effective stress at the bottom of a clay layer with permeable top and impermeable bottom due to haversine repeated loading

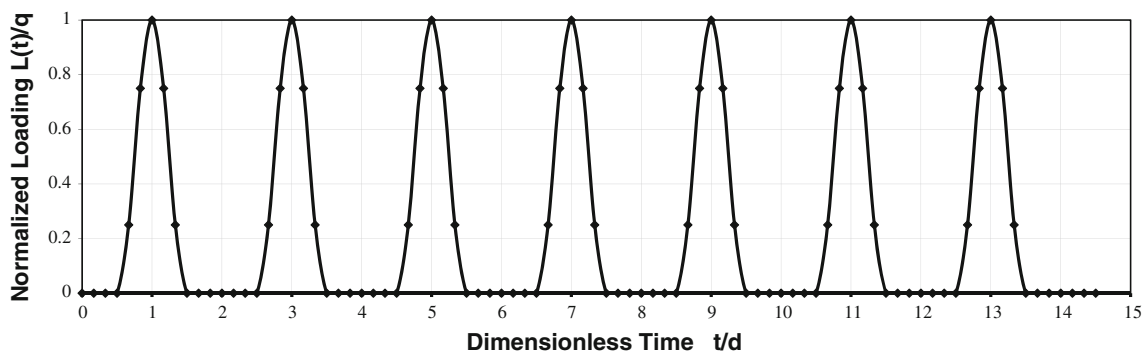


Fig. 6 Haversine repeated loading with rest period (case $R/d = 1$)

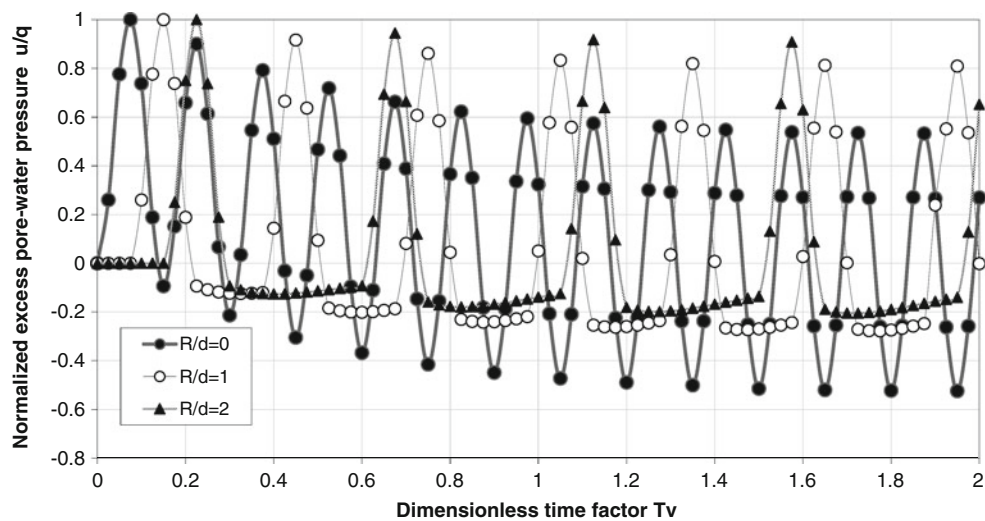


Fig. 7 Effect of rest period of haversine repeated loading on the time variation of “excess” pore-water pressure at the bottom of a clay layer with permeable top and impermeable bottom

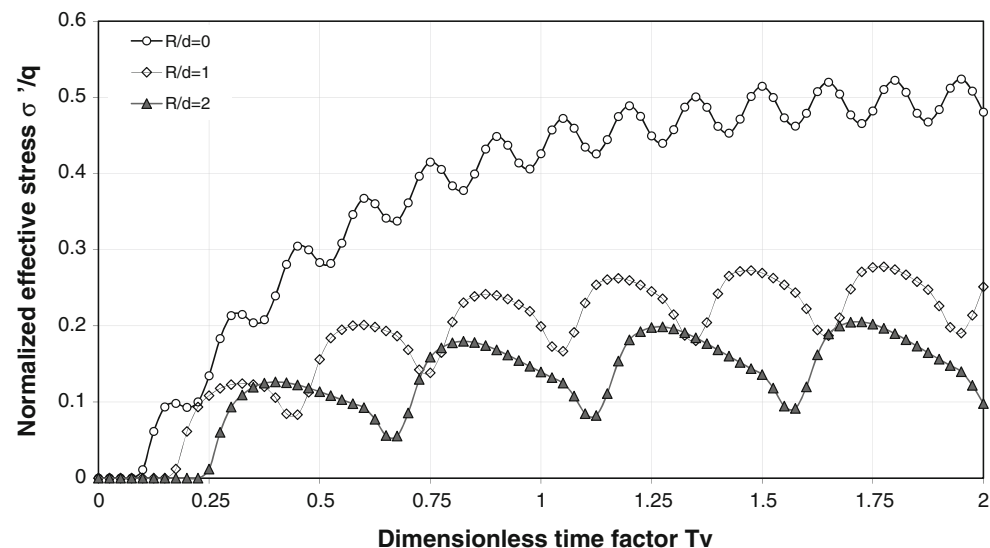


Fig. 8 Effect of rest period of haversine repeated loading on the time variation of effective stress at the bottom of a clay layer with permeable top and impermeable bottom

the maximum absolute value of negative pore-water pressure becomes smaller by increasing the rest period.

However, the number of cycles required to achieve ‘stationary state’ decreases with increasing the rest period, as it is about 5 for the case of non-zero rest period compared with 8 for $R = 0$.

Figure 8 shows the effect of rest period on the time variation of effective stress. It is quite obvious from this figure that the effective stress increases with time but with more pronounced fluctuation when compared with the case of no rest period ($R = 0$). However, the maximum effective stress achieved decreases with increasing R/d ratio,

indicating that the consolidation process becomes slower by increasing the rest period. It is also worth mentioning that for non-zero rest period, a ‘steady’ state is achieved after the fifth cycle, indicating that the rest period tends to decrease the number of cycles required to achieve the steady state.

9 Conclusions

The main conclusions of this work can be summarized as follows:

1. Although the haversine loading is always positive, the ‘excess’ pore–water pressure developed during one-dimensional consolidation oscillates changing from positive to negative and vice versa. The absolute value of the amplitude of this excess pressure decreases gradually with time until a steady state is achieved.
2. Regarding the excess pore-water pressure and effective stress, a steady state is achieved after about eight cycles for the case of haversine repeated loading without rest period and after the fifth cycle for non-zero rest period.
3. The effective stress and hence the bearing capacity of the soil increase with time although showing some fluctuations but without changing sign. This fact is independent of the length of rest period.
4. The ‘excess’ pore-water pressure isochrones can be positive, negative or consisting of two parts, namely positive and negative.
5. An increase in the rest period of the haversine repeated loading decelerates the one-dimensional consolidation process. The maximum effective stress for non-zero rest period becomes much less than that for no rest period.
6. The number of cycles required to achieve the ‘steady-state’ conditions decreases with increasing the rest period. Five cycles are sufficient to achieve this state for a non-zero rest period.

Acknowledgments The first author thanks German Academic Exchange Service (DAAD) for funding his stay as a guest professor with the second author in 2009/2010.

References

- 1 Baligh MM, Levadoux JN (1978) Consolidation theory for cyclic loading. *J Geotech Eng Div, ASCE* 104(4):415–431
- 2 Barksdale RG (1971) Compressive stress pulse times in flexible pavements for use in dynamic testing. *Highway research record* 345, HRB, pp 32–44
- 3 Conte E, Troncone F (2006) One-dimensional consolidation under general time-dependent loading. *Can Geotech J* 43:1107–1116
- 4 Crank J (1993) The mathematics of diffusion, 2nd edn. Clarendon Press, Oxford
- 5 Favaretti M, Soranzo M (1995) A simplified consolidation theory in cyclic loading condition. In: Proceedings of the international symposium on compression and consolidation of clayey soils, Japan, pp 405–409
- 6 Geng X, Xu C, Cai Y (2006) Non-linear consolidation analysis of soil with variable compressibility and permeability under cyclic loadings. *Int J Numer Anal Methods Geomech* 30:803–821
- 7 Guan S, Xie K, Iiu AE (2003) An analysis on one-dimensional consolidation behaviour of soils under cyclic loading. *Rock Soil Mech* 24(5):849–853
- 8 Hsu T, Lu S (2006) Behavior of one-dimensional consolidation under time-dependent loading. *J Eng Mech* 132(4) ASCE
- 9 Huang YH (1993) Pavement analysis and design. Prentice-Hall Inc., Englewood Cliffs
- 10 Kreyszig E (2006) Advanced engineering mathematics, 9th edn. Wiley, Singapore
- 11 McLean DB (1974) Permanent deformation characteristics of asphalt concrete. Ph.D. dissertation, University of California, Berkeley
- 12 Mitchell JK (1993) Fundamentals of soil behaviour. Wiley, New York
- 13 Olson RE (1977) Consolidation under time-dependent loading. *J Geotech Eng Div ASCE* 103(GT1):55–60
- 14 Razouki SS, Al-Zayadi A (2003) Design charts for 2-D consolidation under time-dependent embankment loading. *Q J Eng Geol Hydrogeol* 36(3):245–260
- 15 Terzaghi K, Fröhlich OK (1936) Theorie der Setzung von Tonschichten. Franz Deutike, Leipzig
- 16 Terzaghi K (1925) Erdbaumechanik auf bodenphysikalischen Grundlage. Franz Deutike, Leipzig und Wien
- 17 Terzaghi K (1943) Theoretical soil mechanics. Wiley, New York
- 18 Wylie CA, Barret LC (1985) Advanced engineering mathematics. McGraw-Hill Book Company, London
- 19 Zimmerer M (2009) Identifikation konstitutiver Parameter von weichen feinkörnigen Böden: Beitrag zum Konsolidationsverhalten von Ton. PhD-thesis, Fakultät Bauingenieurwesen, Bauhaus-Universität Weimar, Germany